Fermi National Accelerator Laboratory

FERMILAB-Conf-92/232

High Energy Elastic and Diffractive Scattering

Shekhar Shukla

Fermi National Accelerator Laboratory
P.O. Box 500, Batavia, Illinois 60510

August 1992

Presented at the *International Conference on Physics in Collisions*,
Boulder, CO., June 9-12, 1992

Disclaimer

HIGH ENERGY ELASTIC AND DIFFRACTIVE SCATTERING

Shekhar Shukla
Fermi National Accelerator Laboratory
Batavia, IL 60510
U.S.A.

Abstract

The developments in high energy pp and $p\bar{p}$ elastic scattering in the last 30 years are summarized. The Regge pole model and the geometrical models are reviewed and their agreement with experimental data discussed. The experimental method for measuring the total cross section and the ratio of the real to the imaginary part of the forward elastic scattering amplitude, ρ, is described. The assymptotic behavior of the total cross section at high energy is dicussed in the light of the new results on $p\bar{p}$ elastic scattering at $\sqrt{s}$=1.8 TeV. Predictions from geometrical models and Regge phenomenology are compared with experimental data. The 2-gluon model of the Pomeron by Low and Nussinov is discussed. Future measurements on elastic pp and $p\bar{p}$ elastic scattering are discussed.

The data on high energy hadron scattering during the last decade comes from $p\bar{p}$ scattering. The experimental result that has perhaps attracted the most attention in the last decade is the measurement of ρ, the ratio of the real to the imaginary part of the forward elastic scattering amplitude for $p\bar{p}$ scattering at $\sqrt{s}$=540 GeV by experiment UA4 at CERN[1]. After an introduction to the subject of elastic and diffractive scattering, we review the developments in the field before the UA4 measurement. We briefly describe the Regge model and some geometrical models for high energy elastic scattering and total cross sections. Then we describe the experimental method for the measurement of small angle elastic scattering at a modern pp or $p\bar{p}$ collider. This is followed by a statement of how the experimental data on elastic and soft diffractive scattering, including those on $p\bar{p}$ elastic scattering after the ρ measurement by UA4, agree with various parameterizations of the total cross section. We finally discuss some theoretical predictions and then state our conclusions.

1 INTRODUCTION

We list some general experimental observations about hadron scattering at high energy.

1) The total cross section for any pair of hadrons varies very slowly with energy (see figure 1) and the behavior for the various hadrons is very similar.

2)The total cross sections for the scattering of various hadron pairs, $\sigma_{tot}(pp)$,$\sigma_{tot}(\pi p)$, e.t.c obey the additive quark rule (to $\approx$10%),

$$\sigma_{tot}(AB) = n^A n^B \qquad (1)$$

where $\sigma_{tot}(AB)$ is the cross section for the hadrons A and B and n^A and n^B are the numbers of quarks in A and B respectively.

3)At small values of the 4-momentum transfer squared ($|t|<0.15(Gev/c)^2$), the differential elastic cross section, $d\sigma/dt$, varies as exp(bt), where b is a constant (fig. 2).

4) A dip is observed in pp scattering (fig. 2) at larger values of $|t|(\approx 1\ (Gev/c)^2)$.

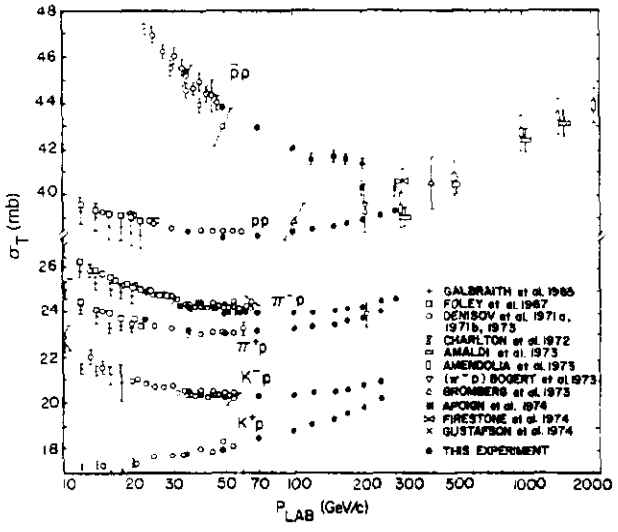

Figure 1 Total cross sections for hadron scattering[2].

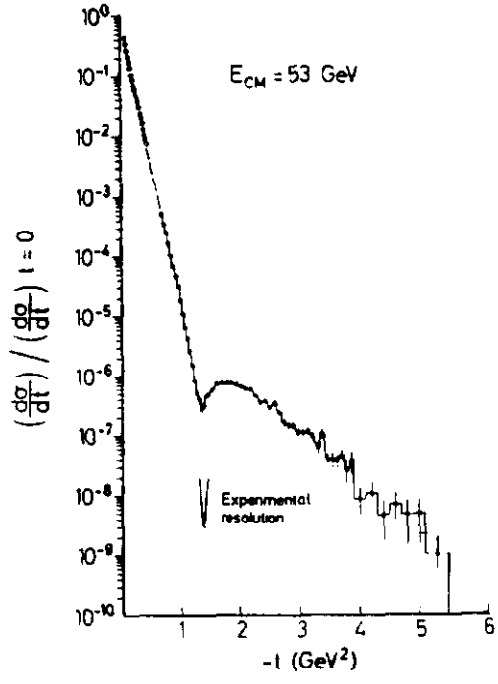

Figure 2. Differential elastic cross section for pp scattering at $\sqrt{s}$=53 GeV[3].

5) The ratio of the differential diffraction dissociation cross section for small $|t|$ and large x (Feynman x), to the differential elastic scattering cross section,

$$R = \frac{d^2\sigma / dt\, dx}{d^2\sigma_{el} / dt} \qquad (2)$$

for a particular hadron dissociating on various target hadrons, is independent of the target hadron, i.e., the diffractive vertex factorizes.

A requirement for any theory of hadron scattering is an ability to explain the observations listed above. For a model of hadron scattering to be successful, it should reproduce these observed characteristics. We do not presently have any accurate theoretical predictions for diffractive scatterting from QCD. This is because diffractive scattering involves processes with very small 4-momentum transfers - usually smaller than the QCD mass scale. Hence perturbative QCD is not very successful in describing it. However, some basic assumptions of analyticity and crossing symmetry for the scattering amplitude and the unitarity of the scattering

matrix, have led to some successful predictions in this field. According to the assumption of analyticity, the 2-body reaction,

$A + B \rightarrow C + D$

is described by an analytic function A(s,t) of the Mandelstam variables, the center of mass energy, s, and the 4-momentum transfer squared, t, the variables being considered as complex variables. Crossing symmetry means that the t-channel and u-channel reactions,

$A + \overline{C} \rightarrow \overline{B} + D$

and

$A + \overline{D} \rightarrow \overline{B} + C$

are described by analytic continuations of A(s,t).

We have a more detailed phenomenological description of diffractive processes provided by Regge theory. Some geometrical models also have been very successful in reproducing the experimental data.

2 HISTORICAL REVIEW

In the 60's it was widely believed that the total cross sections for hadron scattering are constant (with change in energy) at high energy. Then the pp cross section was measured in the early 70's in the range $\sqrt{s}$=20-60 GeV at the Intersecting Storage Rings (ISR) in CERN[4]. Contrary to expectations at the time, it was found to be rising with energy. The question then was whether the cross section rose assymptotically, and if it did, how fast did it rise. There was also the question about the assymptotic behavior of the difference in the pp and the $p\overline{p}$ cross sections, $\Delta\sigma = \sigma(p\overline{p}) - \sigma(pp)$.

The measurement of ρ, the ratio of the real to the imaginary part of the forward elastic scattering amplitude, at the ISR[5] followed that of the total cross section. Since the scattering amplitude is an analytic function of t, the real part of the forward elastic scattering amplitude is related to an integral over the imaginary part

through the dispersion relations. Hence knowledge of the real part helps in determining the behavior of the total cross section.

There are also some assymptotic theorems based on the analytic properties of the scattering amplitude, that constrain the high energy behavior of hadron scattering, and provide guidelines in attempts to answer questions about the behavior of total cross sections. One such theorem places an upper bound (Froissart bound) on the growth of the total cross section for a pair of hadrons[6]. It states that,

$$\lim_{s \to \infty} \sigma \leq \left(\frac{\pi}{m_\pi^2}\right) \mathrm{Log}^2(s/s_0) \approx (60\,\mathrm{mb})\,\mathrm{Log}^2(s/s_0) \qquad (3)$$

where s_0 is an unspecified constant usually taken to be of the order of the hadron mass scale, i.e., $\approx$1 GeV. According to another theorem[7], if the pp or $p\bar{p}$ cross sections grow as $\mathrm{Log}^{\gamma}(s/s_0)$, the difference between them cannot grow faster than $\mathrm{Log}^{\gamma/2}(s/s_0)$.

In an attempt to answer the questions about the total cross sections, Amaldi et al[5] fit all the existing experimental data on total cross section and ρ for pp and $p\bar{p}$ scattering simultaneously, using dispersion relations. Motivated by the Froissart bound and probably the Regge pole model, they parametrized the cross section for $pp/p\bar{p}$ scattering as follows,

$$\sigma_{pp/p\bar{p}} = a + b\,E^{-\mu} -/+ c\,E^{-\nu} + d\,\mathrm{Log}^{\gamma}s \qquad (4)$$

with a, b, c, d, μ, ν and γ as free parameters. They obtained, a=27.0±1.0, b=41.9±1.1, c=24.2±1.1, d=0.17±0.08, μ = 0.37± 0.03, ν = 0.55±0.02 and γ =2.1± 0.1. The experimental data and the curve corresponding to the best fit are shown in figures 3a and 3b. The fit indicated that the cross section rises assymptotically as $\mathrm{Log}^2 s$, that is, as the highest power of Log s allowed by equation 3. However, it should be noted that the value d=0.17±0.08 is much smaller than the multiplicative factor of 60 mb in equation 3. The fit by Amaldi et al further predicted a rise in the $p\bar{p}$ cross section through the ISR energy range. When the total cross section and ρ were measured at the ISR[8),9)] for $p\bar{p}$ scattering, they were consistent with the predictions from the fit. The cross section measured by the CERN experiment UA4 at $\sqrt{s}$=546 GeV was also

consistent with the predictions. It should be noted that even though the fit was consistent with $\Delta\sigma$ vanishing at high energy, it did not rule out terms in the scattering amplitude, called odderons[10], that give rise to an assymptotically non-vanishing value of $\Delta\sigma$.

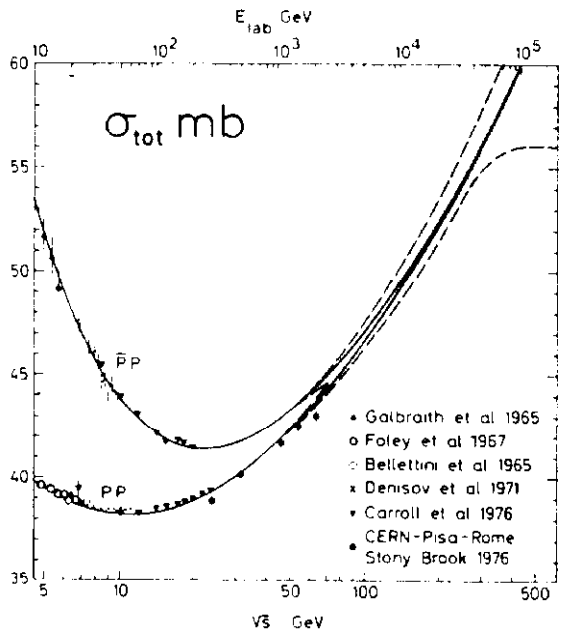

Fig 3a Total cross sections Amaldi fit[5]

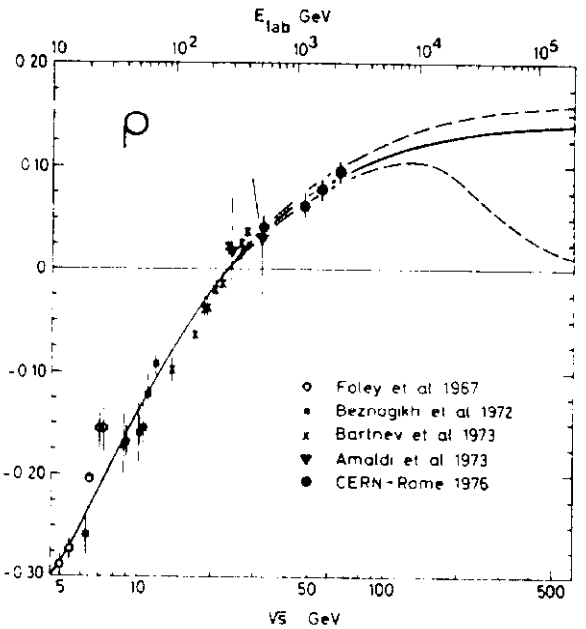

Fig 3b ρ values Amaldi fit[5]

3 THE REGGE MODEL

One of the earlier models used (in the 60's) for elastic scattering and total cross section , was the one particle exchange model in which the two particle scattering, A+B→C+D, results form the exchange of a single particle (see fig 4) . According to this model the elastic scattering amplitude at high energy is given by,

$$A(s,t) \sim \frac{s^j}{t - m^2} \qquad (5)$$

where j is the spin of the exchanged particle. The resulting variation of the total cross section given by,

$$\sigma_{tot} \sim s^{j-1} \qquad (6)$$

The model predicts indefinitely rising cross sections if the exchanged particle has spin greater than unity. In the 60's this was seen as a problem, since at the time, the cross sections seemed to be constant at the highest available energy ($\sqrt{s} \approx 15$ GeV) and were believed to be assymptotically constant with energy.

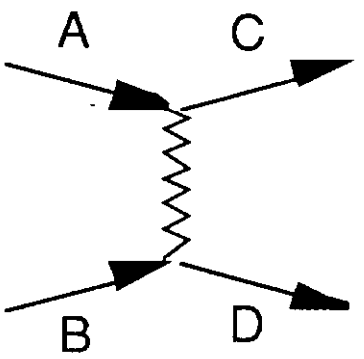

Fig 4 One Particle exchange model.

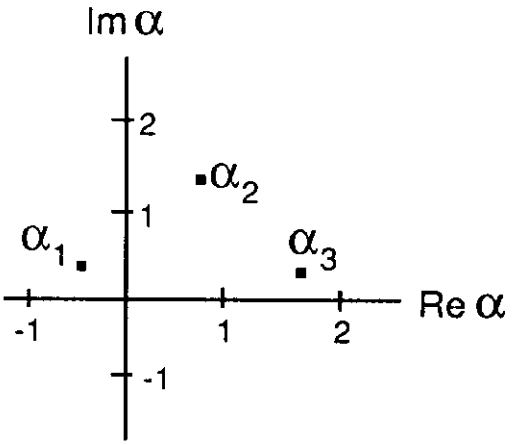

Fig 5 Regge poles in the complex angular momentum plane.

In the Regge pole model which followed, one writes the partial wave expansion for the scattering amplitude as,

$$A(s,t) = \sum_{l=0}^{\infty} (2l+1)\, T(\alpha,s)_{\alpha=l}\, P_l(\cos\theta) \qquad (7)$$

and assumes that $T(\alpha,s)$ is an analytic function of the angular momentum α, considered to be a complex variable, and that the only singularities of the function are simple poles (called Regge poles). As s changes the pole moves in the α-plane describing what is called a *Regge trajectory*. A Regge trajectory passing close to $\alpha=0,1,2,...$ describes a resonance. The trajectories of meson resonances, taken to be straight lines, are shown in figure 6 (Chew-Frautschi plot). The isospin, I, and the charge conjugation number, C, for the mesons on the four trajectories are listed in the figure. The four trajectories are degenerate with the slope $\alpha' \equiv 1$ and intercept $\alpha'(0) \equiv 0.5$.

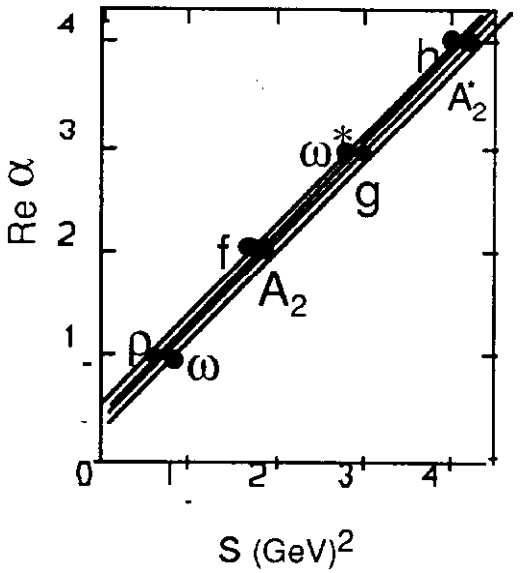

Chew-Frautschi plot
Meson Regge Trajectories

C = -1	I = 1	ρ - g
C = +1	I = 0	ω – ω *
C = -1	I = 1	A_2 - A_2 *
C = +1	I = 0	f - h

Figure 6 Meson Trajectories.

For large s and small | t |, the scattering amplitude A(s,t) for the process,

A + B → C + D,

is determined by Regge trajectories α_i (t) in the crossed channel (t-channel),

$A + \overline{C} \rightarrow \overline{B} + D$

The exchange of a particle of momentum j in the one particle exchange model is replaced by the exchange of a Regge trajectory α(t).

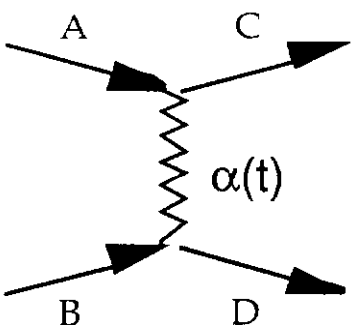

Figure 7 Regge trajectory exchange

The scattering amplitude due to the exchange can be written as[11],

$$A(s,t) = \gamma_{AC}(t)\,\gamma_{BD}(t)\,f(\alpha(t))\left(\frac{s}{s_0}\right)^{\alpha(t)} \qquad (8)$$

where $\gamma_{AC}(t)$ represents the coupling of the trajectory to the particles A and C at the upper vertex, $\gamma_{BD}(t)$ is the coupling to particles B and D and f(t) is a function containing the Reggeon propagator. The exchange of two or more Reggeons gives rise to branch cut in the α-plane [11], called a Regge cut.

If Regge pole exchange is the dominant mechanism at high energy, then, from equation 8, the amplitude at large s is dominated by the trajectory $\alpha(t)$ with the largest intercept at t=0, called the leading trajectory, and the amplitude is given by,

$$A(s,t) \sim h(t)\left(\frac{s}{s_0}\right)^{\alpha(t)} \qquad (9)$$

where s_0 is the hadronic mass scale taken to be ≈1GeV. The total cross section behaves as ,

$$\sigma_t \sim \left(\frac{s}{s_0}\right)^{\alpha(0)-1} \qquad (10)$$

The total hadron cross sections and the forward differential elastic cross sections are observed to vary very slowly at high energy, and the variation is similar for all hadron pairs. The behavior is said to be caused by the exchange of a Pomeron. Here, as in the remainder of this report, we take the word Pomeron to mean the soft pomeron and not the 'hard' pomeron[12]. Opinion seems to be divided on whether the Pomeron is a Regge pole or a Regge cut. We now state an experimental result from single diffractive dissociation that is relevent to the issue.

If the Pomeron is a pole, then we should be able to write the ratio of the single diffractive dissociation cross section to the differential elastic cross section,

$$R = \frac{d^2\sigma / dt\, dx}{d\,\sigma_{el} / dt} \qquad (11)$$

for a hadron h dissociating on a hadron a (see figures 8a and 8b), as,

$$R = \left[\frac{\gamma_{hX}(t)\gamma_{aa}(t)}{\gamma_{hh}(t)\gamma_{aa}(t)}\right]^2 = \left[\frac{\gamma_{hX}(t)}{\gamma_{hh}(t)}\right]^2 \qquad (12)$$

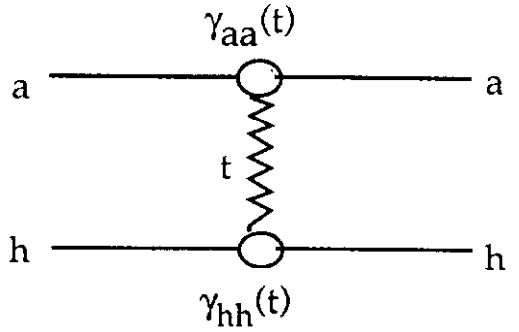

Figure 8a) Elastic Scattering

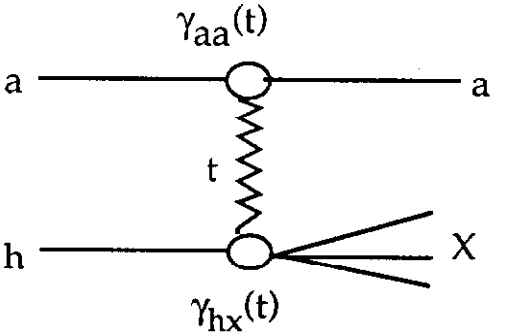

Figure 8b Diffraction Dissociation

We see that when a given hadron dissociates on different target hadrons, the ratio is independent of the target hadron used. The ratio was measured by Ayres et al[13] for protons dissociating in reactions $a+p \rightarrow a+X$, where $a=\pi^{\pm}$, $K^{\pm}$ or $p^{\pm}$ at incident momenta of 140 or 175 GeV. It was found to be the same for the various reactions within experimental uncertainty. The factorization property of the Pomeron coupling has also been tested in other fixed target experiments[14,15] and found to hold. If the Pomeron were a cut it would not necessarily lead to factorizable coupling. Thus the experimental data indicate that it is more likely that the Pomeron is a pole rather than a cut.

The additive quark rule (equation 1) suggests that the pomeron couples to only one quark in each nucleon.

In the small $|t|$ region, the trajectories are expected to be straight lines and we write,

$$\alpha(t) \cong \alpha_0 + \alpha' t \tag{13}$$

Then the elastic differential cross section can be written as,

$$\frac{d\sigma}{dt} \sim F(t) \left(\frac{s}{s_0}\right)^{2\alpha_0 - 2} \exp\left[2\alpha' \log(s/s_0) t\right] \tag{14}$$

The observed elastic scattering distributions show that at t=0,

$$\frac{d\sigma}{dt} \sim e^{bt} \tag{15}$$

where b is a constant called the nuclear slope parameter. This suggests that we can approximate F(t) as,

$$F(t) = F_0 e^{at} \tag{16}$$

Then we can identify the nuclear slope parameter in elastic scattering as,

$$b = a + 2\alpha' \log(s/s_0) \tag{17}$$

The above equation predicts the 'Shrinkage of diffraction peak', which is observed in experiment (see fig 9)

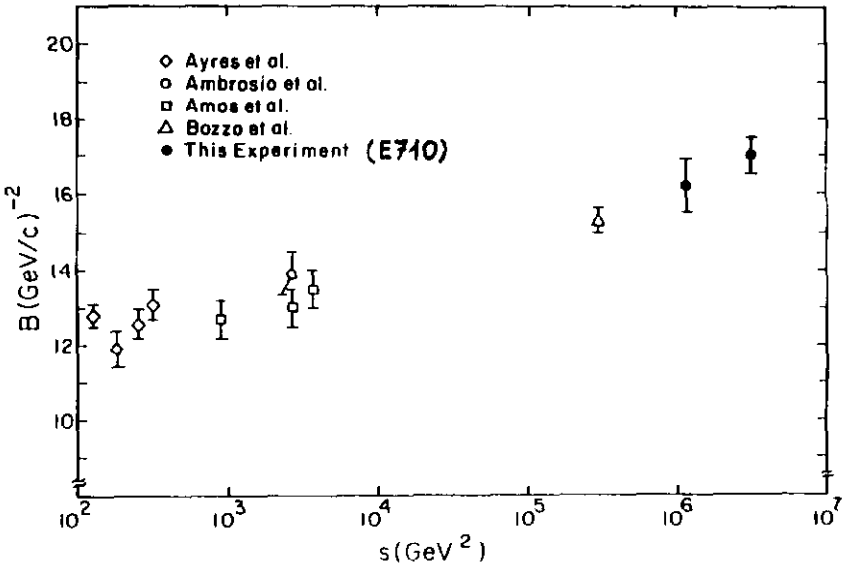

Figure 9 The logarithmic nuclear slope B=d[Log(ds/dt)]/dt

Equation 15 is a good approximation to the behavior of $d\sigma/dt$ only over small ranges of t. This can be seen from the difference in the values of b obtained by fitting over different t-ranges, and from the curvature parameter C in the parameterization of the form,

$$\frac{d\sigma}{dt} \sim e^{bt+ct^2} \tag{18}$$

measured in some experiments. The curve is found to be flatter at larger values of $|t|$. At still larger values of $|t|$ one observes a dip in the differential cross section curve (see figure 2). Lanshoff[16] attributes the larger $|t|$behavior to a Regge cut arising from a two-pomeron exchange, and an odd charge conjugation 3-gluon

exchange (odderon). The Regge cut gives rise to a flatter dependence than the single pomeron exchange and hence is expected to become more important at larger values of $|t|$. The difference between the pp and the $p\bar{p}$ scattering is attributed to the odderon exchange[16),17)].

The total cross sections are rising at the highest energy at which measurements have been made. If a Pomeron dominates the high energy behavior, its intercept should be greater than 1. Using the total cross sections data, Landshoff[16)] finds the intercept to be ≈ 1.085 and the slope to be ≈ 0.25. If the power law behavior of the cross section (equation 10) were to continue indefinitely, it would ultimately violate the Froissart bound. But the energy at which this would happen should be far from that attainable in the foreseeable future. Before those energies are reached, multiple pomeron exchange is expected to change the behavior of the total cross section so that it obeys the Froissart bound.

The exchange of a Pomeron leads to identical behavior for particle-particle and particle-antiparticle scattering. The difference between the particle-particle and particle-antiparticle cross sections is (widely) believed to arise from the exchange of meson trajectories which consists of quark exchanges (see figure 10).

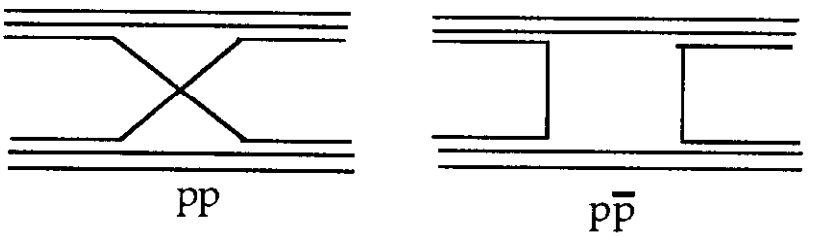

Figure 10. Quark exchange trajectories.

The approximate equality of the measured pp and the np cross sections indicates that the contributions from I=1 trajectories are small. For the leading I=0 trajectories ω (C=-1) and f (C=+1), the intercepts are,

$$\alpha_\omega(0) \equiv \alpha_f(0) \equiv .5 \qquad (19)$$

Their contributions to the total cross section cancel for pp scattering and add for $p\bar{p}$ scattering, resulting in a difference in the cross sections $\Delta\sigma = \sigma(p\bar{p}) - \sigma(pp)$,

$$\Delta\sigma \sim s^{\alpha(0)-1} \tag{20}$$

where $\alpha(0)$ is the intercept of the ρ or ω. Since $\alpha(0)=.5$ we have,

$$\Delta\sigma \sim s^{-0.5} \tag{21}$$

Figure 11 shows the experimental data on $\Delta\sigma$. The data agree well with the variation $1/\sqrt{s}$ expected from equation 21.

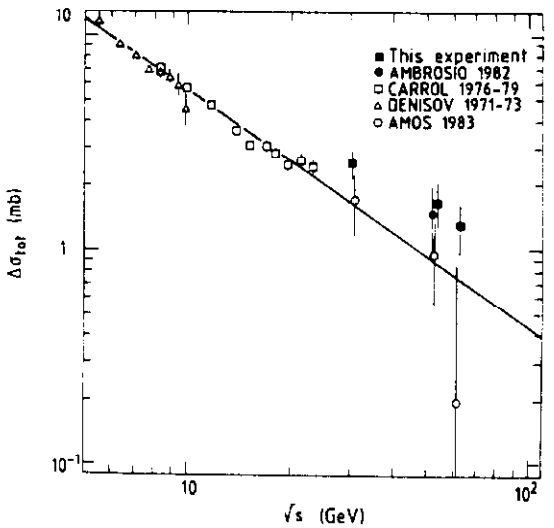

Fig 11 Cross section difference $\Delta\sigma = \sigma(p\bar{p}) - \sigma(pp)$[9]

4 GEOMETRICAL MODELS

The geometrical models of hadron scattering, treat the colliding hadrons as spherical objects scattering off one another.

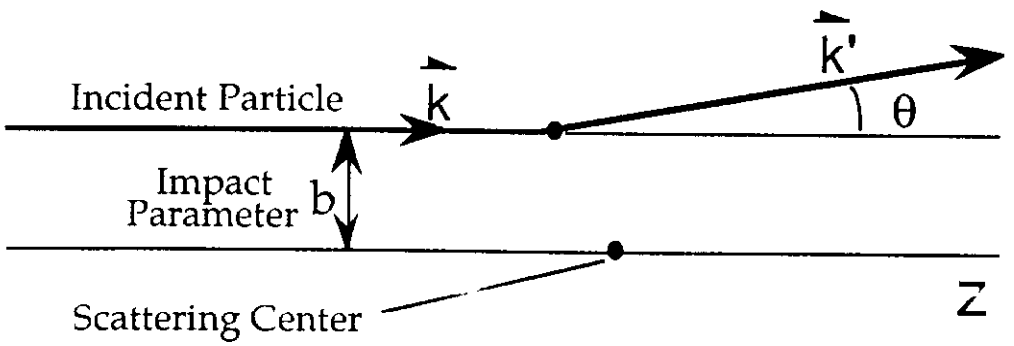

Figure 12. Geometrical Picture

For scattering from a potential that is cylindrically symmetric about the incident particle direction, we write for the scattering amplitude in the impact parameter representation[18],

$$f(\theta) = 2k\int_0^\infty b\, db\, J_0(k\, b\, \sin\theta)\, a(b,s) \tag{22}$$

The geometrical scaling model[19] assumes that,

$$a(b,s) \xrightarrow[s\to\infty]{} a(b / R(s)) \tag{23}$$

where R(s) is an effective interaction radius. In this model, the change in the total and elastic cross sections is due to a change of the interaction radius and the ratio $R=\sigma_{el}/\sigma_{tot}$ is constant with energy for high energy scattering. The ratio was fairly constant through the ISR energy range (figure 13), which was interpreted as evidence for geometrical scaling. But when the ratio was measured at $\sqrt{s}$=540 GeV, it was found to be rising contrary to what one would expect from the model at high energies.

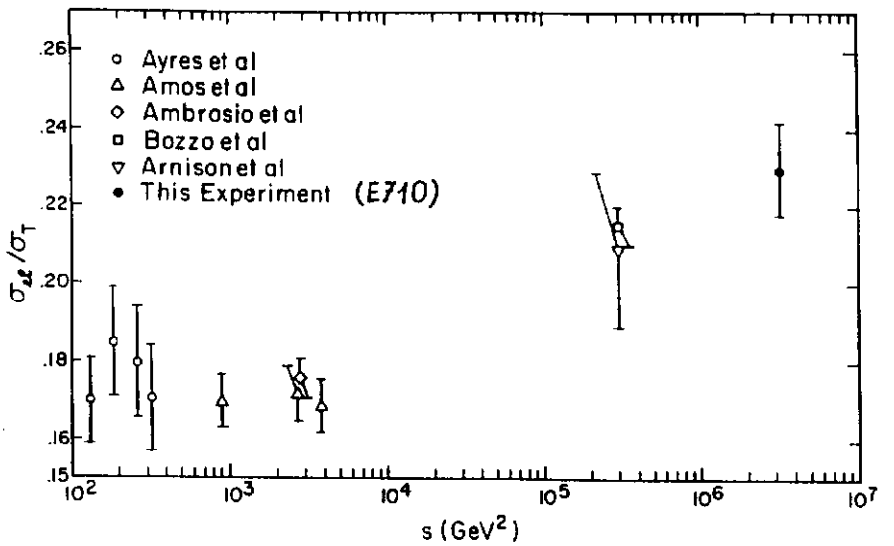

Fig 13 Ratio of the elastic to total cross section.

In the Chou-Yang model[20] one writes,

$$a(b,s) = \frac{i}{2}\left(1 - e^{-\Omega(b)}\right) \tag{24}$$

where $\Omega(b)$ is the opaqueness function and is determined by the matter distributions in the colliding hadrons and their overlap. The matter distributions are assumed to have the same shape as the charge distribution determined from ep scattering, and are used to calculate the shape of $\Omega(b)$. The strength of the interaction is then calculated from the measured value of the total cross section, to obtain the opaqueness function. The prediction of a dip in the differential cross section curve for pp scattering[21], which was later observed when the data became available (fig 2), was a major success for the model.

There are several Chou-Yang type models, in which the opaqueness function is calculated from other considerations than the form factor obtained from ep scattering. The impact picture model of Cheng, Walker and Wu[22] has been particularly sucessful.

5 EXPERIMENTAL MEASUREMENT OF SMALL ANGLE ELASTIC SCATTERING

The hadron-hadron elastic scattering data at $\sqrt{s} > 25$ GeV comes from colliding $p\bar{p}$ beams. The experiments currently active in $p\bar{p}$ elastic scattering are - UA4 at CERN , and CDF and E710 at Fermilab.

5.1 Measurement of Total Cross Section.

There are three methods used in colliding beam machines to measure pp or $p\bar{p}$ total cross sections. One method involves the measurement of the total interaction rate,

$$N_t = N_{el} + N_{inel} \tag{25}$$

where N_{el} and N_{inel} are the elastic and inelastic interaction rates respectively. Then the total cross section is given by,

$$\sigma_t = N_t / L, \tag{26}$$

where L is the luminosity. Most of the elastic scattering is at very small scattering angles. Particles from inelastic scattering emerge at larger angles. The method was used by experiment R210 at the CERN ISR in the 70's. One needs a good luminosity measurement for this method.

Another method involves the measurement of L and the differential elastic event rate dN/dt . One then extrapolates to t=0 to obtain $(dN/dt)_{t=0}$ Then using the optical theorem, the total cross section can be obtained from the equation,

$$\sigma_t = \frac{1}{\sqrt{L}}\left[\frac{16\pi(\hbar c)^2}{(1+\rho^2)}\left(\frac{dN}{dt}\right)_{t=0}\right]^{1/2} \tag{27}$$

The fractional error due to the uncertainty in the luminosity is half of that in the first method. A measurement of dN/dt at small angles is needed to reduce extraplolation error in $(dN/dt)_{t=0}$. The luminosity is calculated by measuring the intensities and shapes of the colliding beams and their overlap.

A third method determines the cross section without a knowledge of the luminosity. Eliminating L form equations 26 and 27, we can write,

$$\sigma_t = \frac{16\pi(\hbar c)^2}{(1+\rho^2)\,(N_{el}+N_{inel})}\left(\frac{dN}{dt}\right)_{t=0} \tag{28}$$

One measures N_{inel} and $(dN/dt)_{t=0}$ and obtains N_{el} by integrating (dN/dt),

$$N_{el} = \int_0^\infty \left[\frac{dN}{dt}\right]_{t=0} e^{-B|t|}d|t| \tag{29}$$

where B is the nuclear slope parameter. Then equation 28 gives the total cross section.

5.2 Measurement of ρ

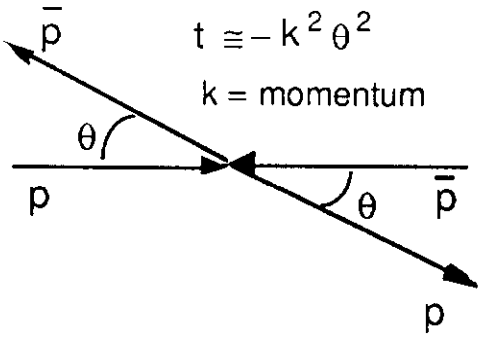

Fig 14 Small angle $p\bar{p}$ elastic scattering

We write for the differential cross section for the near forward pp or $p\bar{p}$ elastic scattering , as for spinless particles,

$$\frac{d\sigma}{dt} = \pi\left|F_c(t)\exp(i\alpha\phi(t)) + F_n(t)\right|^2 \tag{30}$$

where , F_C and F_N are the Coulomb and nuclear scattering amplitudes respectively, α is the fine structure constant, and ϕ is the phase of the Coulomb amplitude relative to the nuclear amplitude. The phase was first calculated by Bethe[23], and has since been calculated by others[24]. The Coulomb amplitude can be written as,

$$F_c = \frac{2\alpha G^2(t)}{|t|} \tag{31}$$

where G(t) is the electromagnetic form factor of the proton. Motivated by the exponential shape of the forward diffraction peak, we write for the nuclear amplitude,

$$F_n(t) = F_n(0)\exp(-B|t|/2) \tag{32}$$

where B is the nuclear slope parameter that describes the forward diffraction peak.

According to the optical theorem,

$$\mathrm{Im}F_n(0) = \frac{\sigma_t}{4\pi} \tag{33}$$

where σ_t is the total nuclear cross section. Substituting equation 33 in equation 32, and writing ,

$$\rho = \mathrm{Re}\,F_n(t) / \mathrm{Im}\,F_n(t) \tag{34}$$

we get,

$$F_n(t) = \frac{\sigma_t}{4\pi}(\rho + i)\exp(-B|t|/2) \tag{35}$$

Using equations 31 and 32 for F_c and F_n in equation 30, we can write,

$$\frac{d\sigma}{dt} = \frac{d\sigma_c}{dt} + \frac{d\sigma_{cn}}{dt} + \frac{d\sigma_n}{dt} \tag{36}$$

where the three terms on the right hand side - Coulomb, nuclear and the interference terms are given by,

$$\frac{d\sigma_c}{dt} = \frac{4\pi\alpha^2(\hbar c)^2 G^4(t)}{|t|^2} \tag{37}$$

$$\frac{d\sigma_n}{dt} = \frac{\sigma_t^2(1+\rho^2)}{16\pi(\hbar c)^2}\exp(-B|t|) \tag{38}$$

$$\frac{d\sigma_{cn}}{dt} = \frac{\alpha(\rho - \alpha\phi)\sigma_t G^2(t)}{|t|}\exp(-B|t|/2) \qquad (39)$$

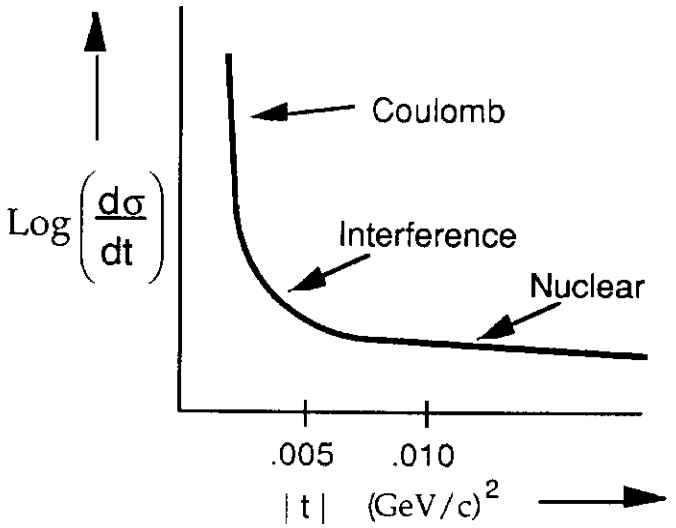

Figure 15 Coulomb nuclear and interference regions (at $\sqrt{s}$ ~ 1TeV)

The Coulomb term dominates at very small 4-momentum transfers (see figure 15), while the scattering is almost entirely nuclear at $|t|$ values larger than $0.01(GeV/c)^2$. In an intermediate t-region, around $t \approx 0.001$ $(GeV/c)^2$ there is a significant contribution from the interference term. Measurements of the differential cross section in this region are needed for the determination of ρ.

The critical factor in the success of an elastic scattering experiment often turns out to be the smallest scattering angles at which it can count elastic events with small backgrounds. The background at small angles is usually due to beam halo, which is a halo of charged particles that surrounds the beam. The extent of the halo depends on the extent of the beam. The part of the beam that determines the halo is the long tails that extend beyond the core, the core being more or less gaussian-shaped . A practice that is often followed to reduce the tails and hence the extent of the halo, is 'scraping'. This consists of introducing metal foils limiting the aperture available to the beam at some point along the beam axis.

5.3 Accessing Small Scattering Angles

Figure 16 shows the projection of the detection setup for a $p\bar{p}$ scattering in the yz plane. If there are no focusing magnets between the collision and the detection points, the minimum angle θ_{min} in the projection is given by,

$$\theta_{min} = Y_{min} / L_{eff} \qquad (40)$$

where Y_{min} is the minimum distance at which the detector can count elastic events and L_{eff} is the distance of the detector from the collision point along the beam-axis.

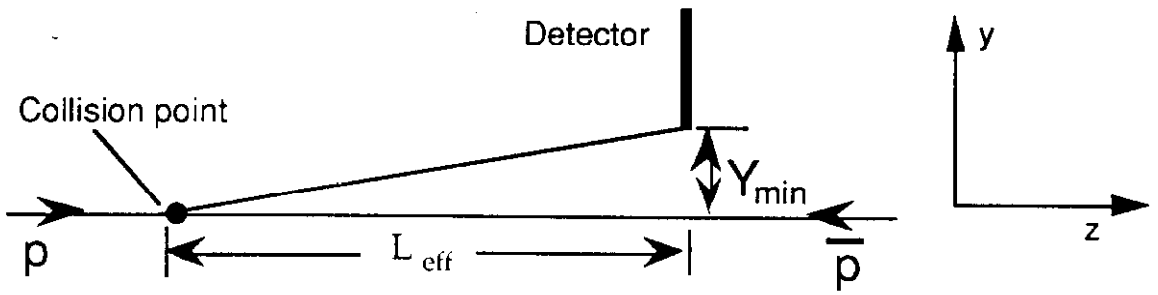

Figure 16 Smallest scattering accessible.

If there are focusing magnets between the interaction point and the detector, the distance L_{eff} in equation 40 is replaced by an effective distance,

$$L_{eff} = \sqrt{\beta_{detector}\ \beta_{collision}}\ \sin\psi \qquad (41)$$

where $\sqrt{\beta_{detector}}$ and $\sqrt{\beta_{collision}}$ are the betatron oscillation amplitudes at the detection and collision points respectively, and ψ is the phase advance between the collision and detection points.

For accessing small scattering angles we need a large L_{eff} and small Y_{min}. So we try to have ψ as close to $\pi/2$ as possible. The beam size at the detector, which determines the extent of the halo background, increases as $\sqrt{\beta_{detector}}$. Since the halo background is what usually decides the smallest distance from the beam at which elastic events can be recorded, $Y_{min} \propto \sqrt{\beta_{detector}}$. Hence one does not reduce θ_{min} by increasing $\beta_{detector}$. Increasing $\beta_{collision}$ does help in reducing θ_{min}. However, this results in a lower luminosity. Thus the demand of a high $\beta_{collision}$ might conflict with other experiments that need a high luminosity. A hard scraping to reduce the width of the beam also helps reduce θ_{min}, but again, conflicts with high luminosity

requirements. Elastic scattering measurements sometimes require dedicated runs in which the luminosity is sacrificed to obtain clean data at smaller angles.

Figure 17 shows schematically the setup of the detectors of Fermilab experiment E710, which is a typical setup for an elastic scattering experiment at a colliding beam facility. The experiment recorded elastic scattering data in a t-range $0.001<|t|<0.6$ $(GeV/c)^2$ at $\sqrt{s}=1.8$ TeV, and in a lower $|t|$-range at some lower energies. The active region of the detectors was ≈2 mm from the beam. It measured the total cross section and ρ at 1.8 TeV.

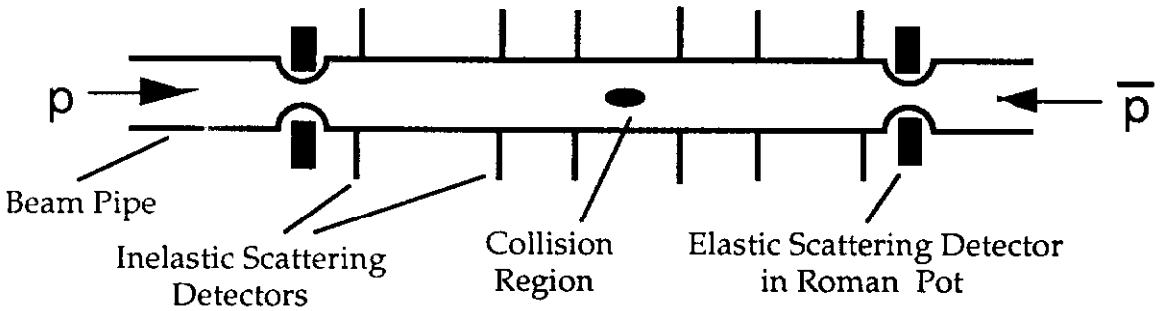

Figure 17 E710 Apparatus (Schematic Representation)

6 THE UA4 ρ-VALUE AND THE MEASUREMENTS AT $\sqrt{s}$ = 1.8 TeV

We now review the recent experimental results in $p\bar{p}$ scattering from CERN at $\sqrt{s}=546$ GeV and Fermilab $\sqrt{s}=1.8$ TeV. The experimental data on total cross sections and ρ, including the total cross section measured at $\sqrt{s}$ = 546 GeV were consistent with the Amaldi predictions (equation 4), and with other models that had the cross sections rising smoothly. In 1987 experiment UA4 at CERN announced their measurement of the ρ value at $\sqrt{s}=546$ GeV[1]. The measured value did not agree with fits using the conventional parameterizations. The predictions arising from these parameterizations were lower by more than twice the experimental uncertainty in the measured value.

A reasonable agreement was obtained if one allowed for an odderon that caused the difference in the pp and $p\bar{p}$ cross sections to grow assymptotically as

Log(s), while the average cross section grew as $Log^2(s)$[25]. The odderon parameterization had been consistent with the data in the past, but so were the conventional parameterizations, and the odderon was not widely believed to be a strong possibility. With the UA4 result on ρ, we had a situation where the conventional parameterizations were inconsistent with some experimental data and the odderon parameterization was not - a situation which would have the odderon merit more serious consideration. There were also several new models that were put forward to explain the unexpectedly high ρ-value. These models interpreted the high ρ as an indication of a new threshold signifying the onset of new phenomena.

The total cross section[26),27)] and ρ[26)] for $p\bar{p}$ scattering have been measured recently at Fermilab at 1.8 TeV. Figure 18 shows the experimental data with a curve corresponding to a conventional parameterization[28)] of the scattering amplitude, i.e., with no threshold or odderon, and with the cross section rising as Log(s) at high energy.

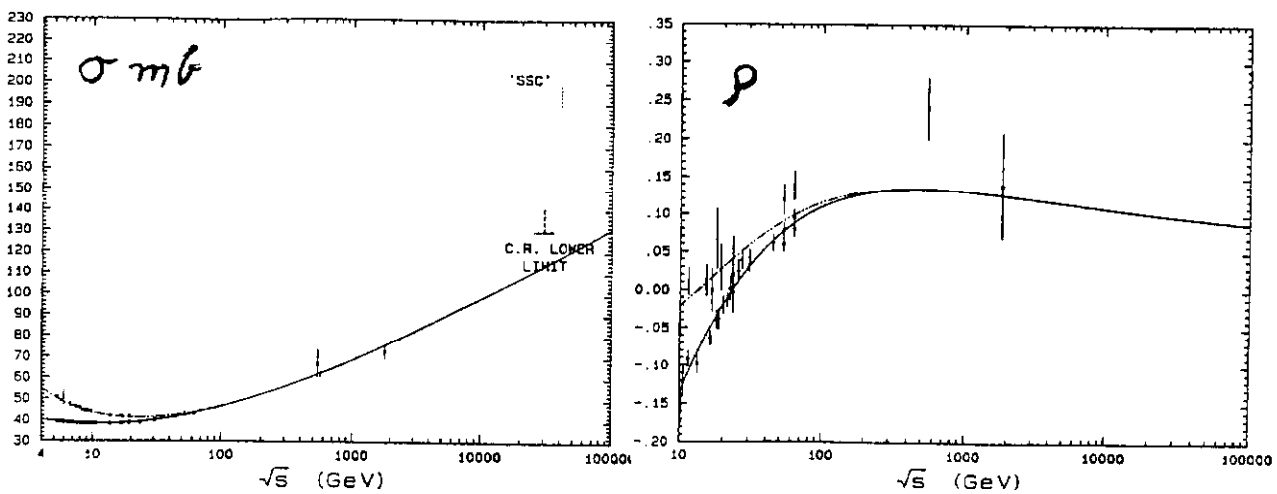

Figure 18 Conventional parameterization[28)].

Fig 19 shows the curve using the odderon parameterization of reference 25. Figures 20 and 21 show fits from reference 29 with thresholds in the scattering amplitude at

$\sqrt{s}$=1.1TeV and 520 GeV respectively. The conventional parameterizations do not agree with the UA4 ρ–value.

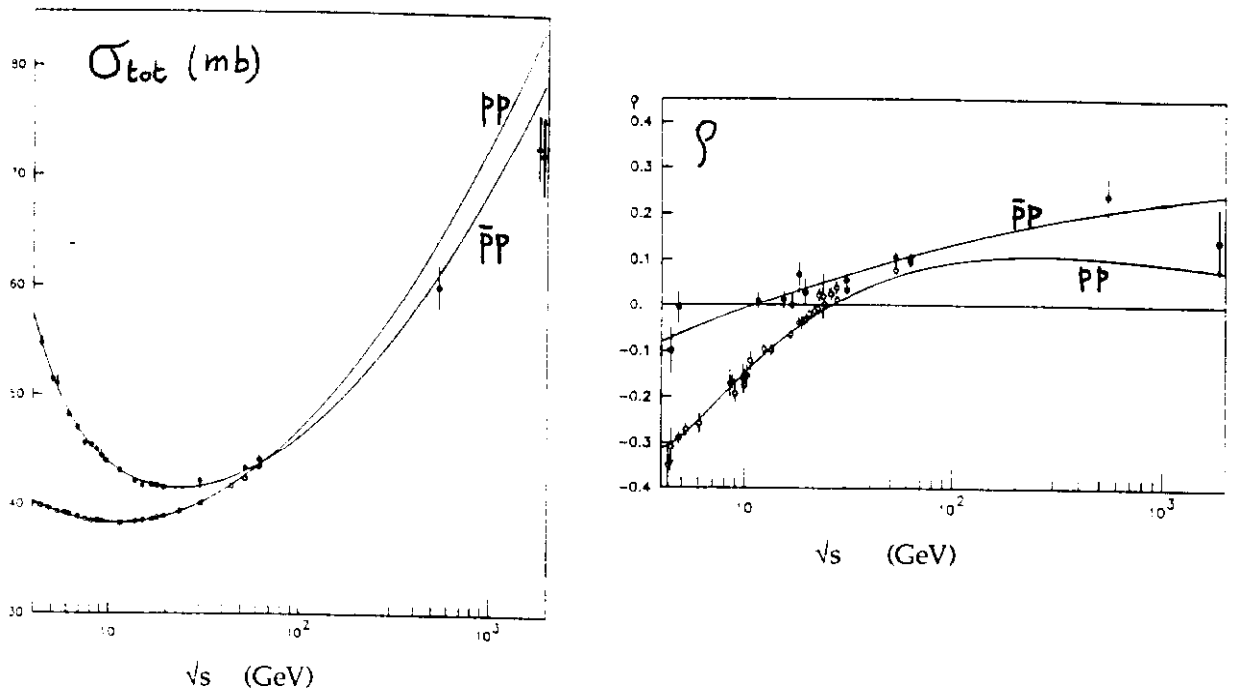

Figure 19 Parameterization with a an odderon[25].

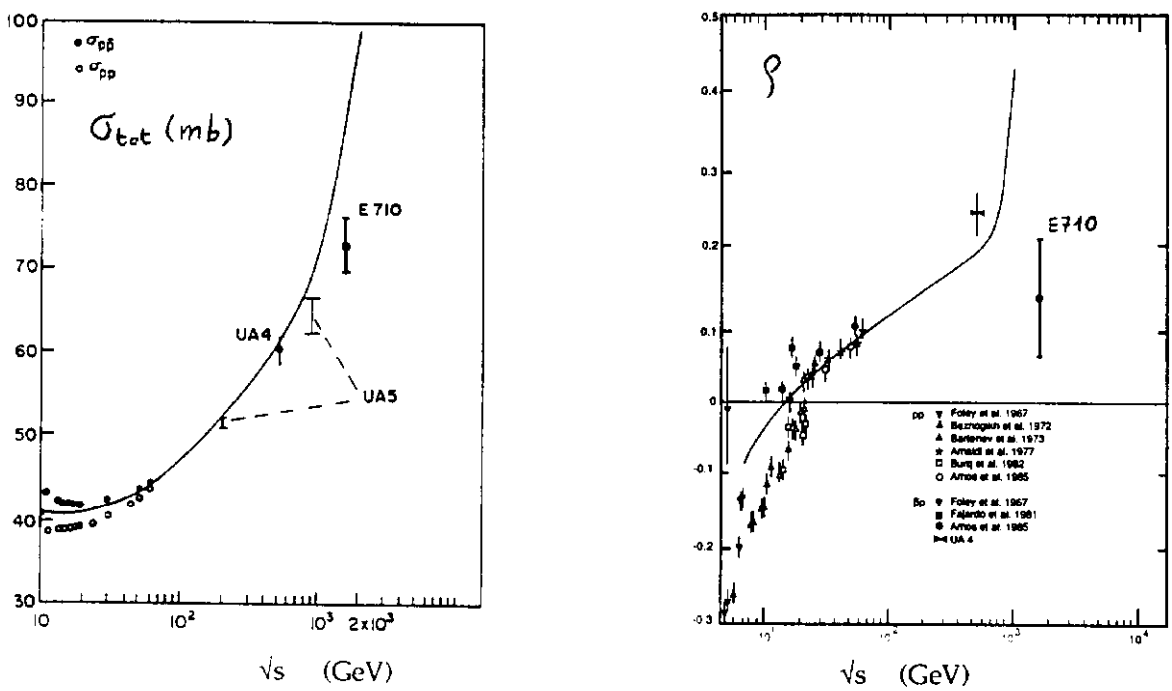

Figure 20 Parameterization with a threshold at $\sqrt{s}$=1.1TeV[29].

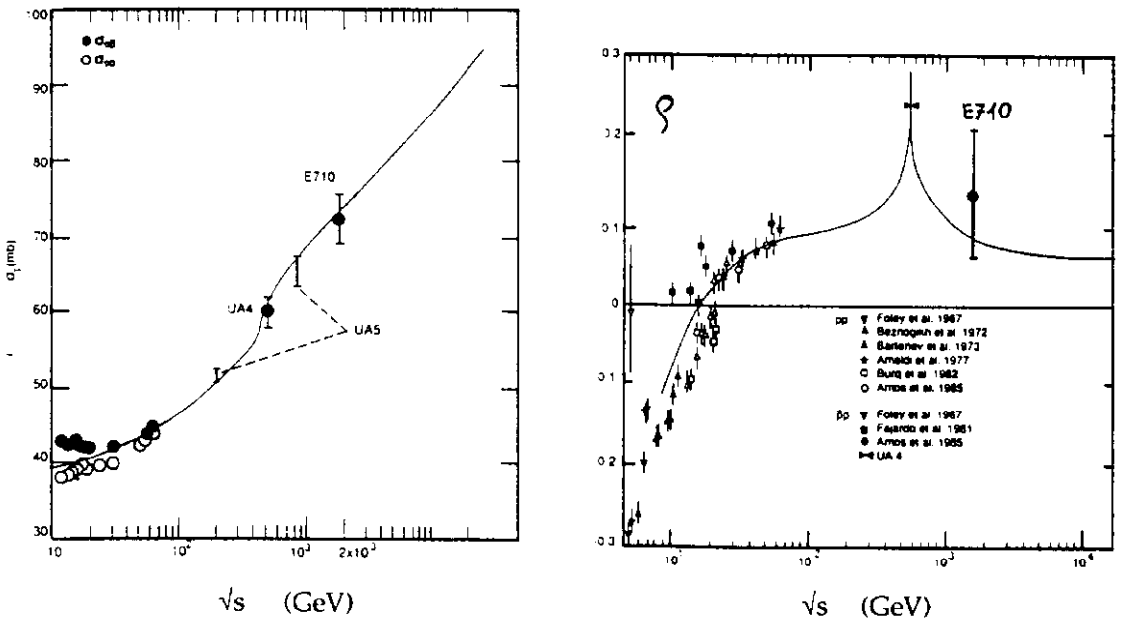

Figure 21 Parameterization with a threshold at $\sqrt{s}$=520 GeV[29].

The parameterizations with a threshold in the scattering amplitude do not agree with the measured total cross at $\sqrt{s}$=1.8 TeV unless the threshold is very close to $\sqrt{s}$=546 GeV. The odderon parameterization agrees better with the UA4 ρ-value than the conventional parameterizations but yields a cross section at $\sqrt{s}$=1.8 TeV that is considerably higher than the measured value.

7 THEORETICAL PREDICTIONS

The experimental data on total cross section and ρ at $\sqrt{s}$=1.8 TeV agree well with the predictions by Bourrely and Soffer[30] using the impact picture.

Donnachie and Landshoff[16] use a Regge picture to describe diffractive scattering. They are able to reproduce the data on forward elastic scattering and total cross sections for pp and $p\bar{p}$ scattering quite well with the exchange of a single Pomeron, which is a Regge pole with intercept ≈1.085 and slope ≈0.25, and of meson trajectories. They describe larger |t| data including the dip region using a double pomeron and an odderon exchange (see figure 22). The total cross section

and ρ curves corresponding to the predictions from this Regge picture and from the geometrical pictures, (for example Bourrely and Soffer[30] look very similar to those shown in figure 18.

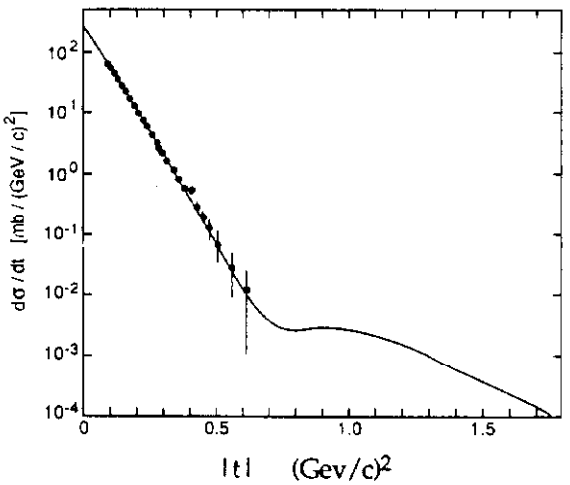

Figure 22 Landshoff[16] prediction for dσ/dt at √s=1.8 TeV

There are some recent calculations for diffractive scattering using QCD. Since all hadron pairs have similar high energy behavior, independent of their flavour, and all known meson trajectories have intercept=.5, Pomeron exchange is usually taken to consist of gluon exchanges. Low and Nussinov[31] proposed a model of the bare pomeron, in which the pomeron exchange is pictured as the exchange of a color octet gluon followed by an exchange of another color octet object (gluon or diquark) to leave the final hadrons in a color singlet state (figure 23)

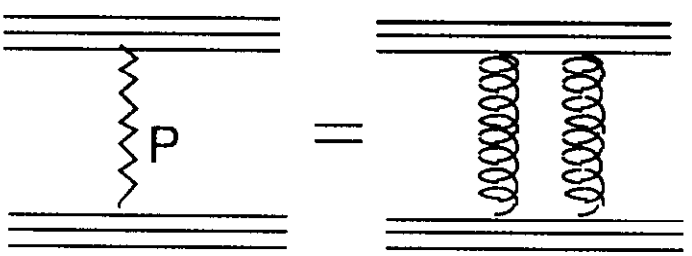

Figure 23 Model for pomeron

Landshoff[32] observed that the characteristics of hadron scattering are described quite well by a pomeron that couples to single quarks like C=+1 isoscalar photon. The QCD calculations have tried to reproduce this behavior using the 2-gluon exchange model. Calculations with perturbative QCD using the model of Low and Nussinov, give the correct order of magnitude for the total cross section[33]. Richards[34] finds that such a calculation does not produce a factorizable coupling for the Pomeron, and does not reproduce the observed behavior of the elastic differential cross sections at small $|t|$.

Landshoff and Nachtman[35] proposed that confinement removes the pole in the perturbative gluon propagator at $k^2=0$ and causes the two gluon exchange to behave like the observed Pomeron. Cudell and Ross[36] have found a new solution to the Dyson-Schwinger equation in which the pole in the gluon propagator was replaced by a softer singularity, hence offering theoretical justification for the idea of Landshoff and Nachtman.

8 CONCLUSIONS

The experimental data on total cross sections and ρ for high energy pp and $p\bar{p}$ elastic scattering, with the exception of the UA4 ρ value, agree well with the conventional models. The UA4 ρ measurement is approximately two and a half times the quoted experimental uncertainty from the predictions. There are almost equal contributions to this uncertainty from statistical and systematic errors. We now investigate the two possibilities :

1) *The true value of ρ at 546 GeV is in agreement with the conventional models.* It is difficult to decide how to treat systematic errors since they do not follow the normal law of errors. That is why it is advisable to keep them as small as possible (sometimes at the expense of statistical accuracy). The quoted systematic error in the UA4 ρ–value itself consists of two comparable contributions added in quadrature[1]. This addition is valid for combining statistical errors but it is difficult to say whether

it is or not for adding systematic errors. If the systematic errors are small relative to the statistical error, their treatment becomes relatively unimportant. If they are big the interpretation of the result becomes more subjective. If we treated the UA4 ρ–value as having an uncertainty of 0.04, all of it statistical in nature, we would conclude that there is only a small probability (~1%) that a correctly performed measurement gives an answer as high as 0.24 (the UA4 value).

2) *The conventional explanations are not valid.* Then the real description of the data might include something like the odderon. However, the odderon parameterization does not agree well with all of the experimental data either (gives too high a cross section at $\sqrt{s}$=1.8 TeV). Then there is the possibility of the threshold implying new physics[29]. But unless there is some other independent evidence of the new phenomenon, it is difficult to consider it a strong possibility. If the threshold parameterization is not considered a possibility, it is unlikely that the true value of ρ at $\sqrt{s}$=540 GeV and the true value of the total cross sectionat $\sqrt{s}$=1.8 TeV lie close to the measured values.

UA4 is in the process of making a second measurement of ρ at 540 GeV, more accurate than the first. It is expected to help resolve the issue of odderons and thresholds. It should be noted that the difference between the ρ predictions is not very large, for example, predictions from the conventional and the odderon parameterizations differ by only $\approx$0.06. So, even after the measurement, we might not have as clear a picture as we would like. Fermilab experiment E811 intends making another more accurate measurement of ρ at $\sqrt{s}$=1.8 TeV. There are also some tentative plans to measure elastic scattering at future accelerators, namely the LHC at CERN, RHIC at the Brookhaven National Laboratory and the SSC.

The prediction[37] from odderon exchange for the difference $\Delta\sigma = \sigma(p\bar{p}) - \sigma(pp)$ at the LHC ($\sqrt{s}$=17 TeV) is $\approx$-6 mb. If the pp and $p\bar{p}$ cross sections are measured at the same machine with the same equipment and procedure, it is possible to measure the difference in the cross sections accurately enough to settle the question of the

odderon. It is not clear at this stage whether there will be both pp and $p\overline{p}$ interactions at the LHC to make such a measurement possible.

It is probable that the choice between the vastly differing parameterizations of the total cross section discussed above will be clearer after the measurements on pp and $p\overline{p}$ elastic scattering expected at CERN and Fermilab in near future. After that clarification, we might still be left with a plethora of models of hadron scattering, all of them consistent with the high energy data, which are predominantly on pp and $p\overline{p}$ elastic scattering. The process of improving our understanding of physics phenomenon involves elimination of hypotheses with the use of experimental data. If there is a dearth of data with small uncertainty, a large number of hypotheses can be consistent with the existing data resulting in an unclear and possibly confusing picture. A more accurate measurement of the forward elastic scattering parameters leads to a clearer picture. Elastic scattering data at larger values of $|t|$ (including and beyond the dip) are also important for testing models. We do not have such data at $\sqrt{s}$=1.8 TeV (Fermilab Tevatron energy). Their importance should not be overlooked in future elastic scattering experiments.

In section 1 we stated that the similarity of the scattering of various hadron pairs, the additive quark rule and factorization of the diffractive vertex, were some of the important characteristics of hadron scattering. They form part of the basis for the conventional pictures of hadron scattering. It is important to check experimentally if these characteristics are unchanged at higher energies, where the total cross sections for pp and $p\overline{p}$ scattering are varying significantly.

9 ACKNOWLEDGEMENTS

I am grateful to Dr.A.R.White for helping me in my attempts to understand the literature on elastic and diffractive scattering, and to Dr.I.Veronesi for assisting in the preparation of this report.

10 REFERENCES

1 UA4 Collab., D. Bernard et al, Phys. Lett. B198(1987)583.
2 A.S. Carrol et al, Phys. Lett. B61(1976)303.
3 A. Bohm et al, Phys. Lett. B49(1974)491.
4 U. Amaldi et al, Phys. Lett. B44(1973)112.
S.R. Amandolia et al, Phys. Lett. B44(1973)119.
5 U. Amaldi et al, Phys. Lett. B66(1977)390.
6 M. Froissart, Phys. Rev. 123(1961)1053.
A. Martin and F. Cheung,*Analytic Properties and Bounds of the Scattering Amplitudes*, Gordon and Breach, New York (1970).
7 R.J. Eden, Phys. Rev. Lett. 16(1966)39
Kinoshita T.,*Perspectives in Modern Physics*, ed., R.E. Marshak(Wiley,New York)1966.
8 R211 Collab., Amos et al., Nucl. Phys. B262(1985)689.
9 R210 Collab., G. Carboni et al, Nucl. Phys. B254(1985)697.
10 L. Lukaszuk and B. Nicolescu, Nuovo Cim. Lett. 8 (1973)405.
11 P.D.B. Collins,*Introduction to Regge Theory and High Energy Physics*, Cambridge, University Press (1977).
12 R. Kirschner, L.N. Lipatov and L. Szymanowsky, Soltan Institute of Nuclear Studies, Report, SI-92-07. Hard pomeron.
13 D.S. Ayres et al, Phys. Rev. Lett. 37(1976)1724.
14 R.L. Cool et al, Phys. Rev. Lett. 47(1981)701.
15 Y. Akimov et al, Phys. Rev. Lett. 39(1977) 1432.
16 Landshoff, Nucl Physics B. (Proc. Suppl) 25 (1990) 129.
17 P. Gauron and B. Nicolescu, Phys. Lett. B258(1991)482.
18 M.M. Block and Cahn, Rev. Mod. Phys. 57(1985)563.
19 J. Dias De Deus, Nucl. Phys. B59(1973)231-236.
20 T.T. Chou and C.N. Yang, Phys. Rev. 170(1968)1591-1596.
21 T.T. Chou and C.N. Yang, Phys. Rev. Lett., 20(1968)1213-1215.
22 H. Cheng, J.K. Walker, T.T. Wu, Phys. Lett. B44(1973)97.
23 H.A. Bethe, Ann. Phys. 3(1958)190.
24 G.B. West and D. Yennie, Phys. Rev. 172(1968)1413.
R.N. Cahn, Z. Phys. C15(1982)253.
25 D. Bernard, P. Gauron and B. Nicolescu, Phys. Lett. B199(1987)125.
26 E710 Collab., Amos et al, Phys. Lett. B243(1990)158.
E710 Collab., Amos et al, Phys. Rev. Lett. B168(1992)2433.
27 CDF Collab., S. White, Nucl. Physics B. (Proc. Suppl) 25 B (1992)19.
28 M.M. Block, K.Kang and A.White, ANL-HEP-PR-91-61, October 1991.
29 K. Kang and A.R. White, Phys. Rev. D42(1990)835.
30 C. Bourrely , J. Soffer, T.T. Wu, Z. Phys. C37(1988)369.
31 F.E. Low, Phys. Rev. D12(1975)163.
S. Nussinov, Phys. Rev. Lett. 35(1975)1286.
32 A. Donnachie and P.V. Landshoff, Nucl. Phys. B231(1984)189.
33 E.M. Levin and M.G. Ryskin, Sov. J. Nucl. Phys. 34(1981)619.
34 D.G. Richards, Nucl. Phys. B258(1985)267.
35 P.V. Landshoff and O. Nachtmann, Z. Phys. C35(1987)405.
36 J.R. Cudell and D.A. Ross, Nucl. Phys. B359(1991)247.
37 B. Nicolescu, Proc. Joint International Lepton-Photon Symposium & Europhysics